Electronic Supplementary Material (ESI) for Lab on a Chip
This journal is © The Royal Society of Chemistry 2013

Supplementary Information

# A Source of Instability in PDMS Microfluidics

Andrea J. Bubendorfer [a,*], Bridget Ingham [a,b], John Kennedy [b,c], W. Mike Arnold [a,b]

[a]Callaghan Innovation Research Limited, PO Box 31310, Lower Hutt 5040, New Zealand.

[b]The MacDiarmid Institute for Advanced Materials and Nanotechnology, PO Box 600, Wellington 6140, New Zealand.

[c]National Isotope Centre, GNS Science, 30 Gracefield Road, Lower Hutt 5010, New Zealand

## Supplemental Information Guide

# 1. Materials and Methods

## 1.1 Fabrication

Microchannel master molds were formed as previously described[1] in SU-8 photoresist (SU-8 2015, MicroChem (Newton, MA)), and rectangular microchannels of dimension 20µm x 100µm x 3cm were cast in PDMS (Sylgard 184 Silicone Elastomer kit, Dow Corning). A 21 µm thick layer of SU-8 photoresist was spin coated onto poly(methylmethacrylate) (PMMA) (Plexiglas gallery® UV100AR, Degussa Plexiglas, Germany) wafers and processed as per standard manufacturer's guidelines[2] in a class 100 cleanroom under yellow light.

The SU-8 films were then patterned to form microfluidic master molds by use of a laser direct writer at 375 nm (LW405A, MicroTech (Palermo, Italy)), or wholly exposed to UV at the i-line ($\lambda = 365$ nm) for 25 s (dose: 10 $mJ.cm^{-2}$). In order to provide enhanced substrate adhesion, the standard post-expose bake (65 °C for 1 min and 95 °C for 2 min) was immediately followed by an additional heating step of 15 minutes at 120 °C. This results in the maximum bond strength between PMMA and SU-8.[3] The mold was developed in SU-8 developer (MicroChem (Newton, MA)) under standard conditions.

For the PMMA master, the same SU-8 original was used to emboss into polycarbonate and then, this reversed image polycarbonate master used to emboss into PMMA.

PDMS slabs and microchannels were produced from the PDMS prepolymer, thoroughly mixed with its curing agent in a 10:1 volume ratio, degassed, then cast onto the prepared SU-8/PMMA mold, and cured for 1 hr at 100 °C unless otherwise stated. Microchannel wells were formed using a biopsy punch (Miltex, 2.5mm). Enclosed devices were formed *via* a PDMS cover plate conformally sealed to the channel piece.

Low Radio Frequency oxygen plasma treatments were carried out with a 125 W, 50 kHz source (Plasma Etch (Carson City, NV)). Each cycle consisted of 8 minutes plasma treatment followed by 5 minutes sonication in deionized water.

## 1.2 Measurement

Electroosmotic flow measurements on PDMS microchannels were determined by the current monitoring method[4] with an applied voltage of 500 V and a combination of 15/20 mM potassium phosphate buffers (pH 7.2, 20 mM) prepared by dissolving potassium hydrogen phosphate (0.53 g, 3 mmol) and potassium dihydrogen phosphate (0.26 g, 2 mmol) in deionised water (250 mL) (18.2 $M\Omega\ cm^{-1}$) supplied by a Barnstead Easypure® RoDI system and filtered immediately prior to use with a 0.45µm regenerated cellulose syringe filter (Sartorius). Each device was measured 5 times in succession.

Rutherford Backscattering spectrometry (RBS) measurements were carried out with a 2.0 MeV $^{4}He^{+}$ ion beam impinging on the samples under normal incidence using a 3 MV Van de Graaff accelerator. The surface barrier detector for measuring the energy of the backscattered particles was mounted at 165°. A low ion current density of 10 $nA.mm^{-2}$ was used to measure the samples non-destructively in less than 15 min.

For synchrotron X-ray fluorescence (XRF) measurements, films of SU-8 with the entire surface exposed to UV using the same conditions as in the lithographic process were used to give a large, flat bulk homogeneous area to observe. PDMS was then cast on the new SU-8 surfaces, and measured for antimony. For a zero control that also allowed estimation of the background signal from the sample chamber, we used PDMS cast on a silicon wafer.

Quantification was possible following measurement of a calibration series of $K_2[Sb_2(C_4H_4O_6)_2]\cdot 3H_2O$ (antimony potassium tartrate (Aldrich)) samples of known concentrations from 0.2 to 2 wt% Sb mixed with boron nitride. Measurements were performed using the XAS beamline at the Australian Synchrotron. The incident X-ray energy was fixed at 30.8 keV - above the Sb K-edge at 30.5 keV. The beam size was approximately 0.4 × 2 mm (v × h). XRF counts were recorded by integrating over the Sb $K_\alpha$ emission line centered at 26.4 keV, and normalized to the incident flux.

The following samples were measured in addition to the calibration standards: masters used for 0, 1, 3, 6, 13, 26 and 39 PDMS castings; PDMS cast on masters that had previously been used 0, 1, 2, 5, 10, 24 and 38 times; PDMS cast and left in contact with the master for 1, 2, 5, 12 and 24 hours at 100 °C; SU-8 films with 0, 1, 3, 5 and 7 plasma treatment cycles as described previously; and PDMS cast on antimony-free silicon for a control.

## 2. SU-8 Structure and processing

SU-8, originally developed as a photoresist for the microelectronics industry, is widely used in the fabrication of microfluidic master molds.[5] This photoresist is the industry standard for lithographic applications both for the high aspect ratios it achieves with its highly branched cross-linked structure, as well as its ability to deposit extremely thick coatings in a single step compared with other photoresists.[6] Essentially, SU-8 (eight denoting the number of cross-linkable epoxide groups per molecule) is the only photoresist capable of forming the desired dimensions necessary for micromaster molds, and photolithography is the prime means of micromaster mold fabrication due to its low cost and rapid prototypability.

Polydimethylsiloxane (PDMS) microchannels are fabricated from SU-8 microchannel master molds lithographically as shown in figure SI.1. SU-8 photoresist is spin-coated onto polymethylmethacrylate (PMMA) as a substrate used to give strong adhesion for long-lasting master molds, then lithographically patterned in the relief of the desired subsequent channel dimensions. During the lithographic process, the SU-8 epoxides cross-link to form a network structure. All uncross-linked SU-8 is washed away during development, leaving a cross-linked pattern containing photoinitiator residues in the produced master mold.

The two part PDMS prepolymer is mixed in a 10:1 ratio of base to curing agent, degassed and cured on the master relief to form a channel piece, then assembled with a cover plate into a microfluidic device.

It is during this curing process, when PDMS is in direct contact with the photomaster, that PDMS can become contaminated with the unwanted photoinitiator residue.

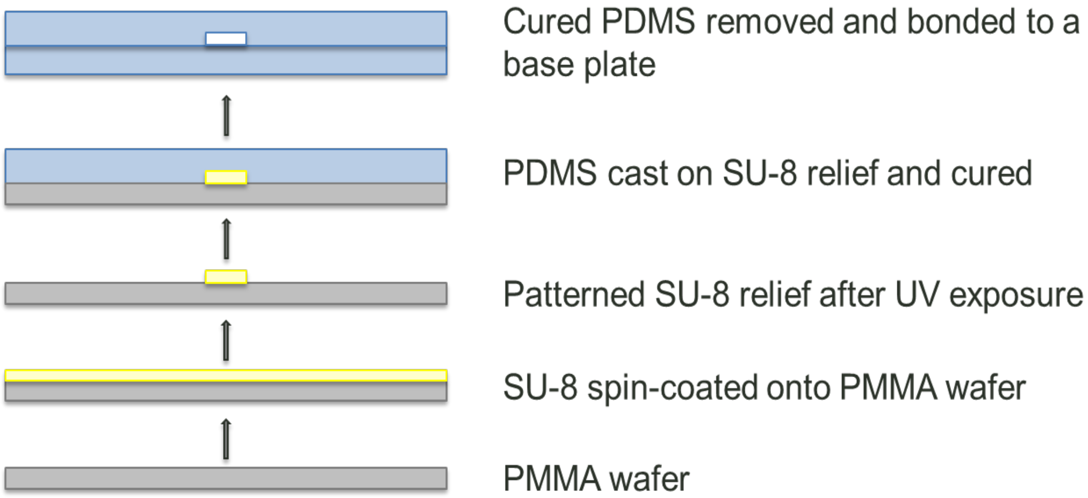

*Figure SI.1: the fabrication protocol whereby PDMS microchannel structures are formed through casting and curing PDMS prepolymer on a photolithographically patterned SU-8 channel relief master on PMMA substrates.*

## 3. Electroosmotic flow

### 3.1 Background

Current monitoring is used to measure microchannel EOF ($\nu_{eof}$ ) rates. A microchannel is filled with a buffer of known concentration at a particular pH and a fixed voltage (V) applied. Once the measured current reaches steady state, the buffer in one of the microchannel wells is replaced with a similar buffer of lower concentration. Upon reapplication of the voltage, the current is traced while the concentration of the solution in the channel equilibrates (indicated by an inflection in the trace). The EOF rate is then determined by dividing the measured channel length ($l$) by the time (t) taken to equilibrate the concentration of the two solutions in the channel, after a steady state current is reached. Electroosmotic mobility (EOM, $\mu_{eof}$) is found by dividing the EOF rate by E, the electric field strength (=V/$l$). A typical example is shown in figure SI.2.

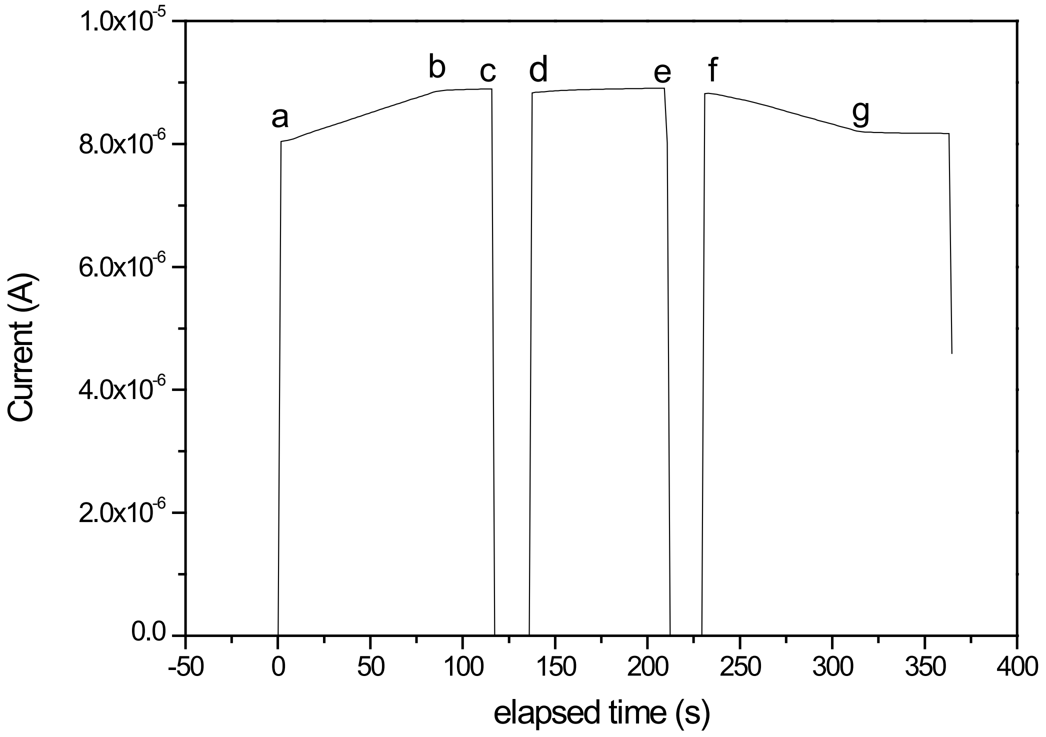

*Figure SI.2: Typical electroosmotic flow rate data demonstrating the time taken for solutions in a microchannel to come to equilibrium.*

Measurement begins at approximately zero seconds (a). The current increases until the solution in the channel equilibrates and becomes stable (b). Shortly after, the voltage is disconnected (c), a replacement solution at the same concentration is added and the voltage reapplied (d) to confirm the current is stable , after which the voltage is again disconnected (e), a fresh solution with lower concentration added and the voltage reapplied (f) and the current falls steadily as the front of lower concentration traverses the length of the channel (g) and the current plateaus thereafter until measurement ceases. The time taken for calculation, t = g-f.

### 3.2 Experimental

We developed a method of creating long-life SU-8 masters by defining the SU-8 structure on poly(methyl methacrylate) (PMMA) wafers, rather than traditional silicon wafers[1]. SU-8 bonds to the PMMA directly, allowing for significantly enhanced adhesion. Because of this, we were able to use SU-8 micromaster molds for many more PDMS casts than previously. Over the course of time with the new long lived master molds, we observed the EOF rates of our PDMS microchannels slowly and erratically reduce.

Observed EOF rates reduced from 0.060 ± 0.002 cm.s$^{-1}$ to a new stable level of 0.033 ± 0.002 cm.s$^{-1}$ from new and well-used masters (after more than a year of regular use, with a minimum of 200 castings assumed), respectively.

Additionally we found that extending the curing time of PDMS microchannels (from 1 to 20 hours) cast on new masters further increased the EOF rate, up to 0.08 ± 0.02 cm.s$^{-1}$ with significantly increased variability, whereas extended contact on a well-used master had no significant effect.

Washing the master (2 hours agitation in DI water) had no effect on the EOF rate of subsequently cast PDMS microchannels. However, flushing the channels prior to use reduced the EOF rate. Pressure flushes (DI water fed through the channel for 15 minutes) and electroosmotic flushes (DI water run through the channel at 500 V until a steady state current was reached) both resulted in a drop in EOF rate from 0.060 ± 0.002 cm.s$^{-1}$ to 0.030 ± 0.002 cm.s$^{-1}$. As with the "hydrophobic recovery" of PDMS (in which surface treatments have a temporary effect; with a new surface regenerating due to migration of the mobile low molecular weight PDMS chains),[7,8] this effect was temporary, working only if carried out immediately before EOF measurement. Similar treatments described as "conditioning" have previously been used[9–11] to stabilize PDMS microfluidic channels by running the filled channel under an applied voltage prior to taking EOF measurements.

Additionally, EOF rate measurements were carried out on a new master mold made with the same channel dimensions, in PMMA. PDMS channels cast on this master, measured EOF rates close to that made on the well-used master and with the flushed channels, at 0.032 ± 0.002 cm.s$^{-1}$.

EOF rates and associated zeta potentials, calculated *via* the Smoluchowski equation are presented in table SI.1

| Channels | EOF rate (cm.s$^{-1}$) | $\zeta$ (mV) |
|---|---|---|
| Cast on well-used master | 0.033 ± 0.002 | -26 ± 2 |
| Cast on new master | 0.062 ± 0.002 | -49 ± 2 |
| Extended contact on new master | 0.08 ± 0.02 | -64 ± 16 |
| Cast on PMMA master | 0.032 ± 0.002 | -25 ± 2 |
| Flushed prior to measurement | 0.030 ± 0.002 | -24 ± 2 |

*Table SI.1. Electroosmotic flow rates ($V = 500$ V, $l = 3$ cm) and zeta potentials of PDMS microchannels cast on SU-8 masters under different conditions. In each case, data are the mean and standard deviations of 5 measurements on a representative device.*

## 4. Rutherford backscattering spectrometry

Rutherford Backscattering spectrometry (RBS) is an ideal technique for analysis of thin films.[12,13] An RBS spectrum can be interpreted using the following key principles: the energy of the elastically scattered beam is proportional to the mass of the target nuclei; the cross-section (yield of backscattered particles) is proportional to the elemental composition of the target material; the incident beam and the backscattered particles lose energy as they pass through the sample. Thus scattering events that occur at a certain depth occur at a lower energy in the spectrum. Elemental concentrations of matrix components and impurities can be investigated as well as depth profiles of almost every element of the periodic table can be measured.

## 5. Synchrotron XRF data processing

Background subtraction was performed using an in-house computer program, written in Java. The Sb peak is located on the side of a Compton scattering feature (see Figure SI.3) and the signals vary from pixel to pixel depending on the pixel location within the detector relative to the sample. Small differences in the sample geometry, e.g. the angle between the sample and detector, or the exact sample positioning, can cause subtle differences in signal. In addition, the signal recorded from each pixel is different in intensity. The computer program performs the following operations:

1. For each pixel, correct for the incident intensity and deadtime, i.e. $Int_{corr} = \frac{Int}{I_0}\frac{ICR}{OCR}$,

where $Int$ is the intensity, $ICR$ is the incident count rate, $OCR$ is the outgoing count rate (all three are different for different pixels), and $I_0$ is the incident X-ray flux. At this step, multiple files can be averaged together.

2. For each pixel, fit the intensity over regions of interest (i.e. either side of the Sb peak) for the sample and background, according to $Int_{sample}(x) = c.Int_{background}(x)$ where $x$ is in the region of interest and $c$ is a constant which is different for each pixel.
3. Subtract the background intensities for each pixel: $Int_{sub} = Int_{sample} - c.Int_{background}$ for all $x$, with $c$ as determined for each pixel in step 2.

4. Sum the subtracted intensities. Bad pixels can be discarded.

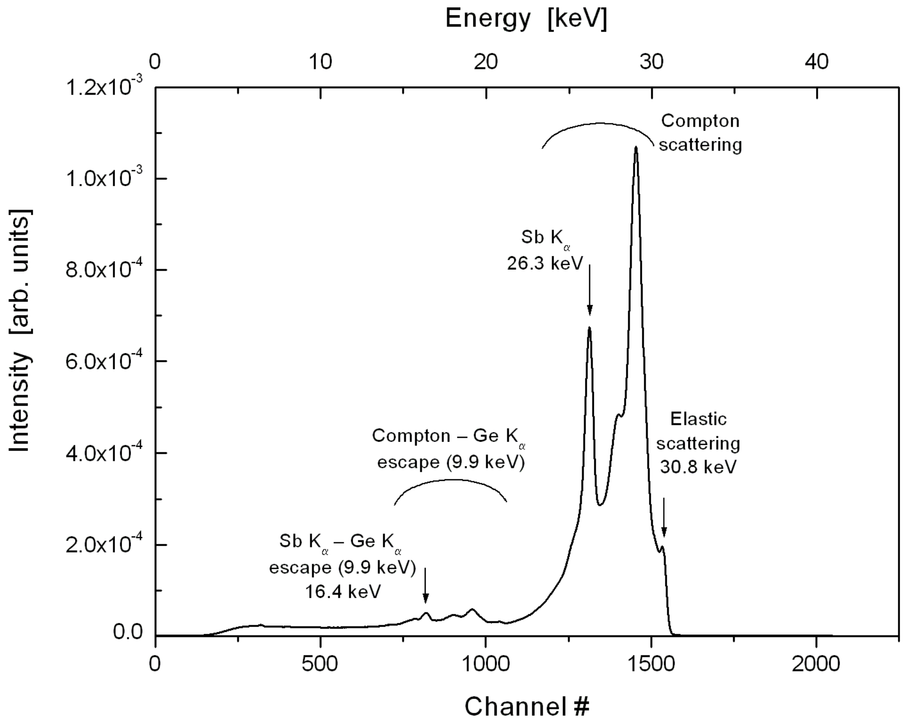

*Figure SI.3. X-ray fluorescence spectrum of 2% Sb standard, plotted against both detector channel number and photon energy, with major features labelled: Compton scattering*[14] *and Ge* $K_\alpha$ *escape peaks from the detector.*[15]

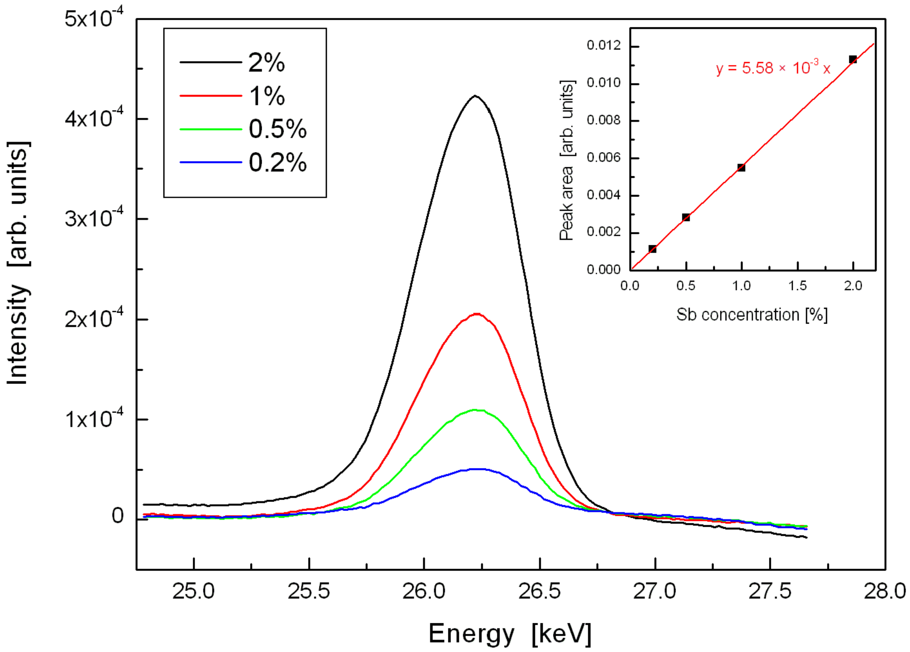

*Figure SI.4: Background-subtracted, normalised X-ray fluorescence spectra of the high concentration standards and calibration plot (inset).*

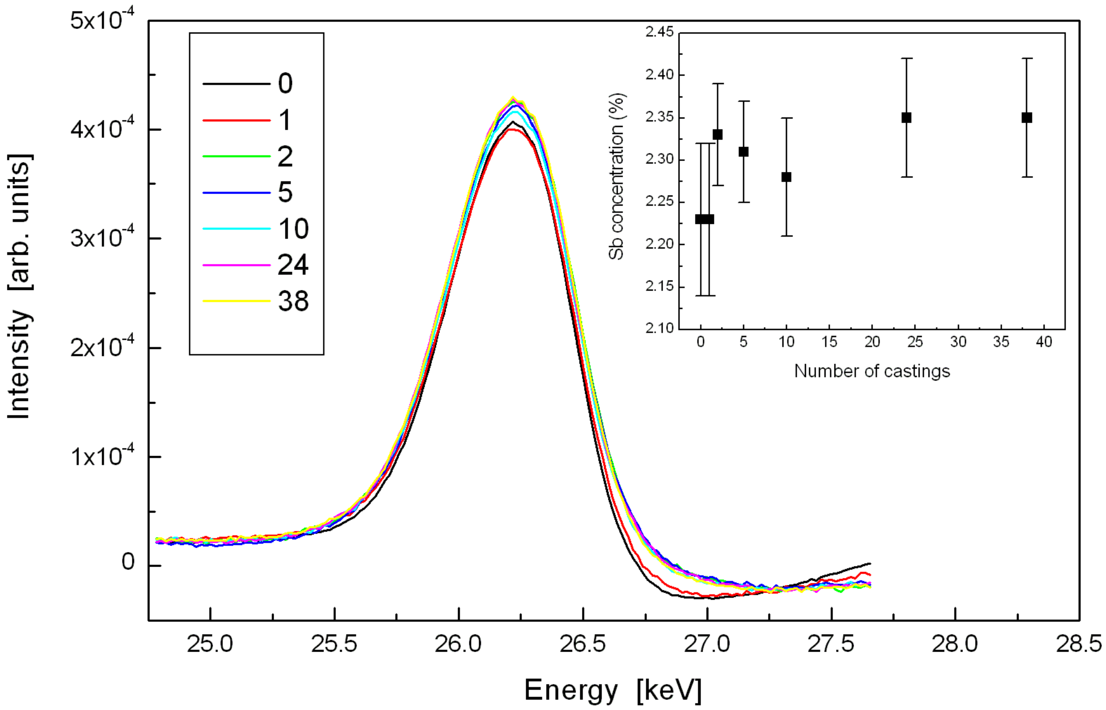

*Figure SI.5: Background-subtracted, normalised synchrotron X-ray fluorescence spectra obtained from masters with different numbers of castings. Inset: Concentration of Sb for the samples shown, calibrated using the calibration curve in Figure SI.4 (inset).*

## 6. Transfer quantities of "hexafluoroantimonic" acid

A transfer of 10Å material per cast is assumed. In one square centimetre this equates to a volume of $1\text{x}10^{-7}$ $\text{cm}^3$. With a density of SU-8 of 1.19 g/$\text{cm}^3$, an equivalent mass of $1.19\text{x}10^{-7}$g is transferred.

Antimony was measured at 2.3% of the SU-8 coating by weight (XRF data), so from a new coating $2.737\text{x}10^{-9}$g of hexafluoroantimonic acid is transferred, with a relative molecular weight of 236.76 g/mol, thus $1.156\text{x}10^{-11}$ mols hexafluoroantimonic acid and the same number of mols of antimony.

Therefore the amount of antimony transferred in a single casting under standard conditions (1 hour at 100 ˚C) from a new master is ~$10\text{x}10^{12}$ atoms/$\text{cm}^2$, below the detection threshold of both RBS and XRF. The quantity transferred from a well-used master would be even less than this. In accordance with this estimate, antimony contamination was not observed in PDMS in these cases, either by RBS or synchrotron XRF. RBS was able to show a discrepancy between the surface antimony concentrations of new and well-used (>200 castings assumed) SU-8 master molds. Synchrotron XRF was only able to detect a transfer after a minimum contact period of 12 hours at 100 ˚C.

## 7. Surface charge density

The Gouy-Chapman theory predicts the following relationship between surface charge density $\sigma$ and surface potential $\psi$ when immersed in a 1:1 electrolyte solution of ionic strength $C$:[16]

$$\sigma/(8N\varepsilon kTC)^{1/2} = \sinh\,(e\psi/2kT)$$

where $N$ is the Avogadro number, $\varepsilon$ is the permittivity, $k$ is the Boltzmann constant, $T$ is the absolute temperature, and $e$ is the electronic charge. If $\sigma$ is expressed in electronic charges per $(\text{nm})^2$ and $C=0.03$ (appropriate for our buffer), and $T=298K$, then inserting accepted values for the other quantities yields:

$$\sigma = 0.1268\,\sinh\,(\psi/51.38)$$

We also note that the size (surface area) of the channel will affect the absolute number of charges transferred, therefore large channel geometries and those with relatively high surface areas would have more total contamination because of that area. In our particular case, the channel size is held constant, therefore this effect has no impact on our results. However in the more general case we expect that the density of transferred surface charge will be independent of the channel surface area. Therefore zeta potential will not be affected, because zeta potential depends on the charge per unit area and not the total charge. [17]

Indeed this is one of the reasons zeta potential is useful in expressing electrokinetic mobilities and for the comparison of different systems.

## 8. Attempted removal of antimony species from PDMS

Flushing a channel prior to use removes the antimony based contaminant (as evidenced by the drop in the measured EOF, Table 1). However this is time-consuming and must be repeated for each device immediately prior to measurement and is thus impractical for widespread use.

It is reported that oxygen plasma treatment in combination with sonication is able to remove antimony species from SU-8.[18–21] The XPS results from the most efficient of these treatments[20] showed a dramatic change of surface concentration of antimony from 0.2 at.% before to 9 at.% after plasma treatment, indicating an accumulation of antimony at the surface. Following a short treatment with water in an ultrasonic bath, the concentration was then reduced to 0.5 at.%. These results suggest that antimony is preferentially brought to, or exposed at, the surface and then removed.

We applied this treatment to new SU-8 micromaster molds twice (noting that the final surface antimony concentration is actually higher than the original level (0.5 at.% *cf* the original 0.2 at.% after one cycle), in order to reduce the antimony concentration at the surface. Following the two cycles of treatment we observed a significantly lower EOF rate of subsequently cast PDMS channels from 0.060 ± 0.002 $cm.s^{-1}$ to 0.036 ± 0.009 $cm.s^{-1}$ (similar to that seen in PDMS channels cast on a well-used master) but also significantly increased variability. It also resulted in the formation of a smaller secondary inflection at 0.05 ± 0.01 $cm.s^{-1}$, indicating the equilibration of another species with a smaller change in concentration (EOF measurements are based on the determination of a single inflection, denoting the time taken for the concentration of the species in the channel to come to equilibrium). The secondary inflection was observed even with only deionised water added to the channel, indicating the species causing it comes from the channel itself, and is therefore likely photoinitiator residue. One of the most exaggerated results is shown as an example in Figure SI.6. Measurements were repeated 30 times with the inflection still visible, though less pronounced indicating some dilution of the contaminant.

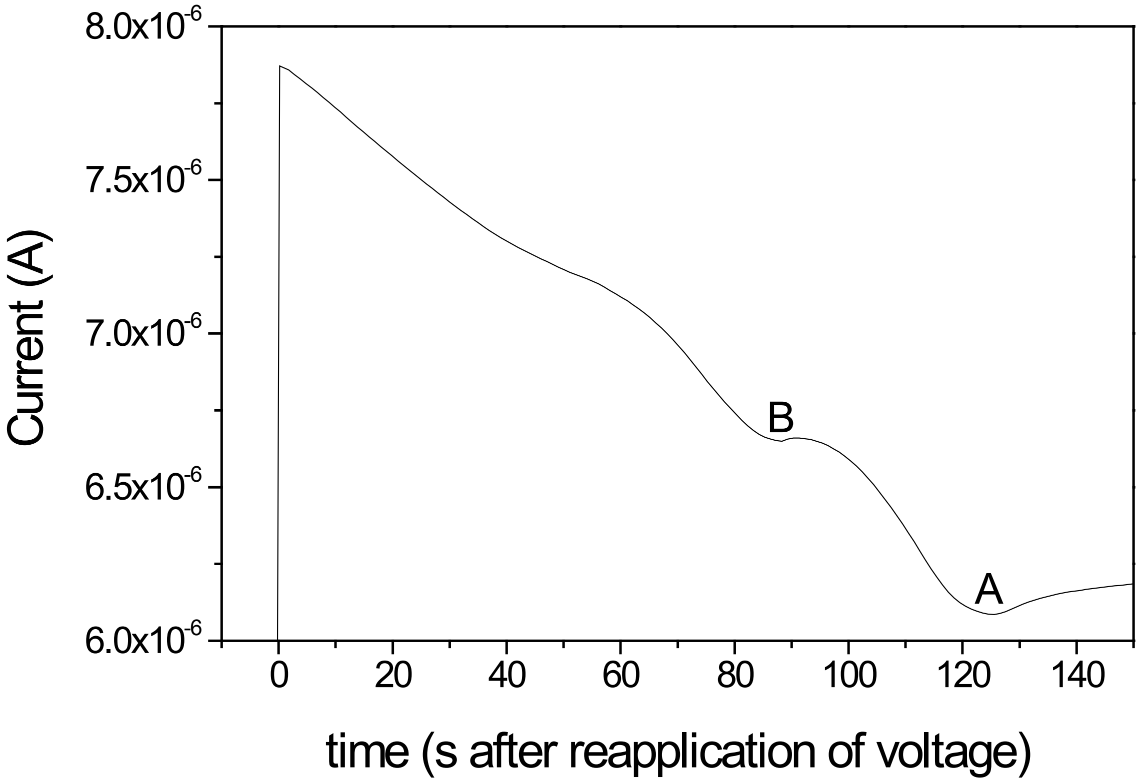

*Figure SI.6. Current monitoring trace indicating the channel EOF rate (dominant inflection at A) and the introduction of a second species in the channel following plasma treatment of the master mold, via a secondary inflection at B.*

The reduction in EOF rates following plasma treatment of SU-8 masters was transient; EOF rates of PDMS channels cast approximately 24 hours after treatment had values similar that of channels cast on untreated masters. This temporary effect may be a due to the mobility of the residue within the SU-8 master resist, as observed by RBS detection of antimony in areas well away from the patterned SU-8.

A series of SU-8 films that underwent 0, 1, 3, 5 and 7 cycles of low RF plasma treatments and sonication were examined for total antimony concentration via synchrotron XRF in order to track the progress of antimony removal. These measurements showed no significant reduction in total antimony content in the masters after seven treatments (Figure SI.7). XANES scans also showed no significant difference in the near-edge spectrum (Figure SI.8). However oxygen plasma treatment is restricted to the surface, XPS measures depths in the range of 1 to 10 nm, while XRF and XANES at the Sb K-edge (~30 keV) probe several mm into the sample (the SU-8 coating itself is 21 µm). Therefore, although antimony species may be removed from the top surface of the film, the vast bulk remains unchanged.

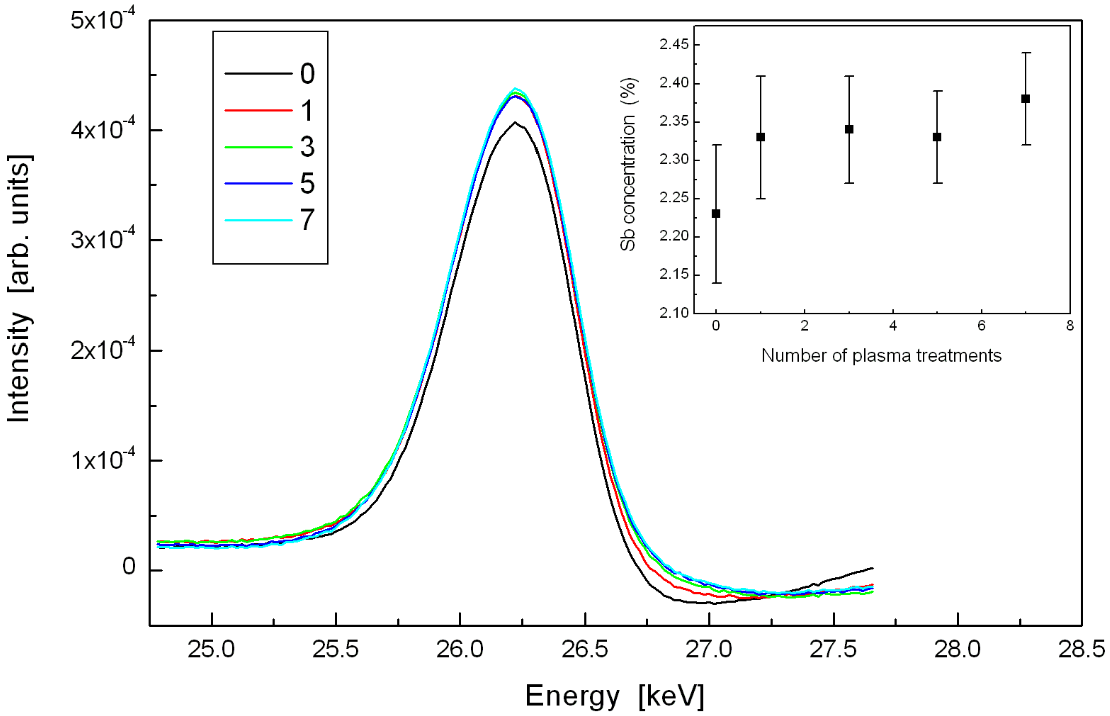

*Figure SI.7: Background-subtracted, normalised synchrotron X-ray fluorescence spectra obtained from masters subjected to plasma treatment. Inset: Concentration of Sb for the samples shown, calibrated using the calibration curve in Figure SI.4 (inset).*

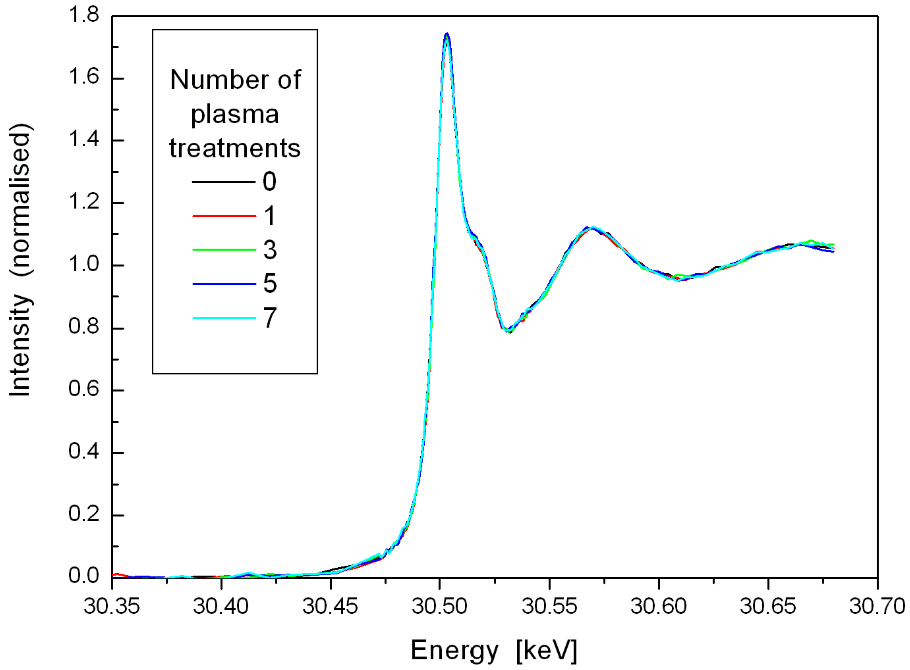

*Figure SI.8: XANES spectra of masters subjected to plasma treatment, showing signals characteristic of octahedral* $Sb^{5+}$.[22]

Repeated plasma treatments on freshly treated surfaces would therefore be unlikely to remove significant amounts of the antimony residue. The residues are extremely difficult to remove from the master mold and to date; the methods we have tested are not viable for practical adoption.

## 8. References

(1) Bubendorfer, A.; Liu, X.; Ellis, A. V *Smart Materials and Structures* **2007**, *16*, 367–371.

(2) SU-8 2000 Permanent Epoxy Resists http://microchem.com/Prod-SU82000.htm.

(3) Bilenberg, B.; Nielsen, T.; Clausen, B.; Kristensen, a *Journal of Micromechanics and Microengineering* **2004**, *14*, 814–818.

(4) Huang, X.; Gordon, M.; Zare, R. *Analytical chemistry* **1988**, 1837–1838.

(5) Makamba, H.; Kim, J. H.; Lim, K.; Park, N.; Hahn, J. H. *Electrophoresis* **2003**, *24*, 3607–19.

(6) Gelorme, J.; Cox, R.; Gutierrez, S. *US Patent 4,882,245* **1989**.

(7) Makamba, H.; Hsieh, Y.-Y.; Sung, W.-C.; Chen, S.-H. *Analytical chemistry* **2005**, *77*, 3971–8.

(8) Bodas, D.; Khan-Malek, C. *Sensors and Actuators B: Chemical* **2007**, *123*, 368–373.

(9) Ocvirk, G.; Munroe, M.; Tang, T.; Oleschuk, R.; Westra, K.; Harrison, D. J. *Electrophoresis* **2000**, *21*, 107–15.

(10) Wheeler, A. R.; Trapp, G.; Trapp, O.; Zare, R. N. *Electrophoresis* **2004**, *25*, 1120–4.

(11) Coltro, W. K. T.; Lunte, S. M.; Carrilho, E. *Electrophoresis* **2008**, *29*, 4928–4937.

(12) J.R. Tesmer, M. N. *Handbook for Modern Ion Beam Analysis*; Materials Research Society: Pittsburgh, 1995.

(13) Kennedy, J.; Markwitz, a.; Trodahl, H. J.; Ruck, B. J.; Durbin, S. M.; Gao, W. *Journal of Electronic Materials* **2007**, *36*, 472–482.

(14) d'Acapito, F.; Golosio, B.; Shimizu, Y.; Scalese, S.; Italia, M.; Alippi, P.; Grasso, S. In *AIP Conference Proceedings*; AIP, 2007; Vol. 882, pp. 375–377.

(15) B. A. Longoni and C. Fiorini *Handbook of practical X-ray fluorescence analysis*; B. Beckhoff, B. Kannigiesser, N. Langhoff, R. Wedell, H. W., Ed.; Springer-Verlag: Berlin, 2006; p. 222.

(16) McLaughlin, S. In *Current Topics in Membranes and Transport*; Kleinzeller, F. B. and A., Ed.; Academic Press, 1977; pp. 71–144.

(17) Hunter, R. J. *Zeta Potential in Colloid Science*; Academic Press: London; p. 1988.

(18) Ferdinand Walther, Polina Davydovskaya, Stefan Zurcher, Michael Kaiser, Helmut Herberg, A. M. G. & R. W. S. *Journal of Micromechanics and Microengineering* **2007**, 524–531.

(19) Hennemeyer, M.; Walther, F.; Kerstan, S.; Schu¨rzinger, K.; Gigler, A. M.; Stark, R. W. *Microelectronic Engineering* **2008**, *85*, 1298–1301.

(20) Walther, F.; Drobek, T.; Gigler, A. M.; Hennemeyer, M.; Kaiser, M.; Herberg, H.; Shimitsu, T.; Morfill, G. E.; Stark, R. W. *Surface and Interface Analysis* **2010**, *42*, 1735–1744.

(21) Vernekar, V. N.; Cullen, D. K.; Fogleman, N.; Choi, Y.; Garcı´a, A. J.; Allen, M. G.; Brewer, G. J.; LaPlaca, M. C. *Journal of Biomedical Materials Research Part A* **2009**, *89*, 138–51.

(22) Tella, M.; Pokrovski, G. S. *Chemical Geology* **2012**, *292-293*, 57–68.